Alternating Frequency Time Domains Identification technique: parameters determination for nonlinear system from measured transmissibility data

Fares MEZGHANI [1,2,*], Alfonso Fernández DEL RINCÓN [2], Mohamed Amine BEN SOUF [1], Pablo García FERNANDEZ [2], Fakher CHAARI [1], Fernando Viadero RUEDA [2], Mohamed HADDAR [1]

[1] *Laboratory of Mechanics, Modelling and Production, National school of Engineering of Sfax, University of Sfax, Sfax, Tunisia*

[2] *Laboratory of Structural and Mechanical Engineering, Superior Technical School of Industrial Engineering and Telecommunications, University of Cantabria, Santander, Spain*

Abstract

In order to better understand nonlinearity, a substantial number of methods have been devoted to extract the stiffness and damping functions. Although most identification methods are based on mathematical models, some promising methods rely mainly on the use of non-parametric techniques, by plotting and adjusting the restoring force to displacement and velocity in the time or frequency domains. However, the identification process in these methods is limited to amplitude-dependence and the identification of nonlinearities that depend on both frequency and amplitude is still required. This is the reason why, in this paper, a nonparametric identification procedure is proposed and an amplitude-frequency-dependent model is developed to predict the system's dynamic behavior under different working conditions. The proposed approach is demonstrated and validated through number of numerical examples with nonlinearities, typically encountered in common engineering applications. Thereafter, this approach is implemented to determine the unknown parameters of a metal mesh isolator from transmissibility data. An application of this technique for identifying the nonlinearity of SDOF system subjected to multi-harmonic excitation is also illustrated.

*Corresponding author. E-mail address: fares.mezghani@gmail.com

Preprint submitted to EUROPEAN JOURNAL OF MECHANICS-A/SOLIDS *September 25, 2019*

Keywords: Frequency-amplitude-dependent parameters, nonparametric identification procedure, transmissibility data, multi-harmonic excitation.

1. Introduction

In many engineering applications, numerous researches have investigated the dynamic properties of nonlinear systems via numerical analysis based on mathematical models. The main objective of the mathematical modeling is to enable the designers to provide a better understanding and characterisation of a real system under different structural and loading conditions. Guo (Guo, 2012) evaluated the transmissibility of nonlinear viscously damped vibration system under harmonic excitation using a new method, based on the Ritz-Galerkin method. It has been implemented to investigate the effect of the damping characterization parameters on this system. Özer and Özgüven (Özer and Özgüven, 2002) used the describing function method to determine the nonlinearity location and evaluate the nonlinearity index by using the complete FRFs of the system (Özer et al., 2009) or the incomplete FRFs (Aykan and Özgüven, 2013). Al-Hadid and Wright (Al-Hadid and Wright, 1989) proposed a method based on the implementation of force-state mapping approach for the location of nonlinearity in discrete lumped-parameter system.

In fact, there are various proposed system identification techniques in order to obtain more accurate mathematical models and correct prediction of dynamic response. Identification methods, based on the linear system theory, have been widely applied in the mechanical vibration for many decays. For nonlinear systems, it is possible to use the model updating techniques which is developed for the linear systems to determine the dynamic characteristics of the system. However, the linearity assumption is not very suitable for identifying the dynamic characteristics of systems with strong nonlinearities, including the friction Coulomb-type. Thus, nonlinear system identification becomes crucial for nonlinear system modeling and several methods have been proposed to detect, localize, determine and identify the nonlinearity (Kerschen et al., 2006).

Some promising identification methods will be briefly reviewed in this paper. A comprehensive review of the time domain methods for nonlinear identification is widely surveyed in the literature (Lin, 1990; Dittman, 2013).

One of the first methodologies of the temporal domain is the restoring force surface method developed by Masri et al. (Masri and Caughey, 1979) to analyze nonlinear systems in terms of their internal restoring forces. Another time domain technique, the Hilbert transform is a well-known technique used in many structural dynamics problems. Feldman showed that it can be applied FREEVIB approach (Feldman, 1994a) based on free vibration and the FORCEVIB approach (Feldman, 1994b) on forced vibration to identify the instantaneous nonlinear model parameters during various types of SDOF excitation. Time domain methods are potentially appropriate for practical engineering applications, however, they are supported by numerical simulation results and still lack the experimental validation. An attempt to exploit the frequency-dependent data has been developed through the use of the Volterra (Volterra, 2005) and Wiener (Wiener, 1942) functional series to address the frequency domain identification of nonlinear systems. Over years, the Volterra series was expanded and the application has been ranging from animal and human biology to electrical and mechanical engineering (Schetzen, 1980). The Volterra series enable the direct generalization of the concept of linear response function and offer more intuitive system interpretation. Unfortunately, the analysis and design of the linear system cannot be used to achieve the nonlinear system characterization in frequency domain.

A critical procedure during the implementation of the parametric methods is the way to obtain nonlinear response of a real structure. Most of these methods are applicable to numerical examples and only a limited number of them are suitable for real nonlinear industrial structures with a complicated model.

For more complex applications, the implementation of non-parametric identification methods, where no priori information about the nonlinearity is required, is efficient; can accurately predict the real behavior by identifying the unknown coefficients through the application of a regression technique. The intend of (Carrella and Ewins, 2011) is to develop a frequency domain method that attempts to extract the stiffness and damping functions from measured data (Carrella, 2012) with no priori knowledge to the type of nonlinearity. The method is particularly suitable for practical applications and implemented to extract the amplitude-dependent parameters of a commercial anti-vibration isolator (Mezghani et al., 2017). Nevertheless, this method is not free of limitations; it may fail when jump occurs and thus will not be two response points measured at the same amplitude of displacement vibration. These errors are introduced especially in the estimation of the damping.

As mentioned previously, the identification methods still require an extension, especially for the non-linearities of damping, depending on both the amplitude and the frequency. There is need and scope to develop a simple technique that allows the extraction of amplitude-frequency-dependent structural nonlinearities from measurements. The Equivalent Dynamic Stiffness Mapping technique was recently proposed by Wang et al. (Wang and Zheng, 2016) and validated numerically and experimentally through examples. This technique has the inherent ability to deal with strong nonlinearities owning complicated frequency response such as jumps and breaks in resonance curves. However, this technique has also some limitations. The steady-state is pre-assumed as the identification is based on deterministic FRFs. Moreover, the primary harmonic response is considered dominant, techniques including sub- or super- harmonics still need further investigation.

Given the fairly limited literature, it can be concluded that there is need to develop a simple technique, which allows the extraction of amplitude-frequency-dependent parameters as well as the stiffness and damping functions from measurements. In this paper, a nonparametric identification procedure is proposed and a amplitude-frequency-dependent model is developed to predict the system's dynamic behavior under different working conditions. The method falls within the category of the single-degree-of-freedom (SDOF) modal analysis methods and the sub- or super- harmonics are considered. The proposed approach is validated through number of numerical examples with nonlinearities, typically encountered in common engineering applications. Thereafter, this approach is implemented to determine the unknown parameters of a metal mesh isolator from transmissibility data. Finally, the assumption considering only the primary harmonic is extended to include the super and sub-harmonics, and an application of this technique to identify the nonlinearity of SDOF system subjected to multi-harmonic excitation is also illustrated.

2. Identification of nonlinear system

2.1. Methodology of identification: Formulation

System identification methods can be classified on the base of their search space:

(a) Parametric methods, which are used in parameter space, seek to determine the value of parameters in an assumed model of the system to be identified.

(b) Nonparametric methods, which are used in function space, produce the best functional representation of the system without a priori assumptions about the system model.

The proposed identification method is considered as a nonparametric method. The equation of motion of the SDOF system Eq. (1) can be expressed in the form of Eq. (2).

$$m\ddot{x}(t) + f(x, \dot{x}) = F_e(t) \tag{1}$$

$$f(x, \dot{x}) = F_e(t) - m\ddot{x}(t) \tag{2}$$

Since the acceleration and force signals are measured for a particular test and the mass is known, the restoring force $f(x, \dot{x})$ can be computed. The displacement $x(t)$ and velocity $\dot{x}$ can be found by direct measurements or through integration of $\ddot{x}(t)$.

In the Harmonic Balance Method (HBM), the response of nonlinear system can be approximated in a truncated Fourier series, such as:

$$x\left(t\right) = d_0 + \sum_{n=1}^{N} A_n \cos\left(n\omega t\right) + B_n sin\left(n\omega t\right) \tag{3}$$

when using only the fundamental harmonic component, the response could be expressed as:

$$x(t) = X_{\cos}\cos(\omega t) + X_{\sin}\sin(\omega t) \tag{4}$$

with the Fourier coefficient calculated as:

$$\begin{aligned} X_{cos} &= \frac{1}{\pi}\int_0^{2\pi} x(t)\cos(\varphi)d\varphi \\ X_{sin} &= \frac{1}{\pi}\int_0^{2\pi} x(t)\sin(\varphi)d\varphi \end{aligned} \tag{5}$$

The Fourier expansion of the first derivation is:

$$\dot{x}(t) = -\omega X_{\cos}\sin(\omega t) + \omega X_{\sin}\cos(\omega t) \tag{6}$$

Due to the absence of cross-product terms, the restoring force is simply equal to the summation of two terms; displacement-dependent term, and velocity-dependent term.

$$f(x, \dot{x}) = K_{eq}x(t) + C_{eq}\dot{x}(t) \tag{7}$$

Therefore, the restoring force can be obtained by Fourier expansion up to the first order as:

$$f(x, \dot{x}) = F_{\cos} \cos(\omega t) + F_{\sin} \sin(\omega t) \tag{8}$$

Replacing $\dot{x}(t)$ and $x(t)$ in Eq.(7) by their expressions in Eq. (4) and Eq.(6) yields:

$$\begin{aligned} f(x, \dot{x}) &= K_{eq}\ X_{cos} \cos(\omega t) + C_{eq}\ \omega\ X_{sin} \cos(\omega t) \\ &+ K_{eq}\ X_{sin}\ \sin(\omega t) - C_{eq}\ \omega\ X_{cos} \sin(\omega t) \end{aligned} \tag{9}$$

Thus (from Eq. (8) and Eq. (9)),

$$\begin{bmatrix} F_{cos} \\ F_{sin} \end{bmatrix} = \begin{bmatrix} X_{cos} & \omega X_{sin} \\ X_{sin} & -\omega X_{cos} \end{bmatrix} \begin{bmatrix} K_{eq} \\ C_{eq} \end{bmatrix} \tag{10}$$

Once the equivalent stiffness and damping, the excitation frequency and the displacement amplitude are obtained, the set of data are plotted as discrete points in the three-dimensional space. Then, the obtained stiffness and damping points are fitted to surface with specific polynomial function over the displacement and the frequency and the mathematical modes are defined.

$$K_{fit} = \sum_{i=1}^{N_1} \sum_{j=1}^{N_2} P_{ij}^{stiff} B_{ij}^{stiff}(X, \omega) \tag{11}$$

$$C_{fit} = \sum_{i=1}^{N_1} \sum_{j=1}^{N_2} P_{ij}^{damp} B_{ij}^{damp}(X, \omega) \tag{12}$$

where P_{ij}^{stiff} and P_{ij}^{damp} are unknown coefficients for stiffness and damping polynomial functions, respectively with N_1 and N_2 presenting the polynomial order. $B_{ij}^{stiff}(X, \omega)$ and $B_{ij}^{damp}(X, \omega)$ are the basic functions, which are power expansion of X and ω.

$$B_{ij}(X, \omega) = X^i \omega^j \tag{13}$$

2.2. Nonlinear equations of motion and their responses to base excitation

As explained in the previous section, there are several types of nonlinearity encountered in the literature and employed to analyze the stiffness and damping models and to identify the unknown parameters. In this paper, three classical numerical examples chosen by Ajjan et al. (Aykan and Özgüven,

2012) and zer et al. (Özer et al., 2009) and one complicated example with combined nonlinearities are studied. The single-degree-of freedom system is shown in Figure 1 where its parameters are taken from (Carrella, 2012) and listed in Table 1.

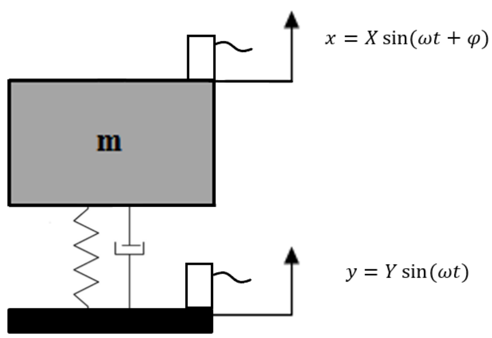

Figure 1. SDOF system of a mass suspended on a nonlinear mount with complex stiffness and under base excitation

During the numerical simulation, direct time integration is carried out for the dynamic equation using the Matlab solver ODE45 which is the 4^{th}-5^{th} orders Runge-Kutta procedure. For each sinusoidal base excitation, responses in 200 cycles are computed with a fixed time step. Only last 100 cycles are taken as the steady-state responses and transformed into the frequency domain in order to ensure the transient components can decay completely. Then, the transmissibility is determined by computing the ratio between the Fourier coefficient of the response and the base excitation amplitude.

2.2.1. Duffing Oscillator

The motion equation of a nonlinear system, examined herein, is written in the form of the Duffing Oscillator as:

$$m\ddot{z} + c\dot{z} + k_1 z + k_{nl} z^3 = \omega^2 m Y \sin(\omega t) \tag{14}$$

where $z = x - y$ presents the relative displacement between the mass and the base and Y represents the amplitude of the base displacement. The response displacement is computed by solving the equation of motion of the system within the frequency range from 9.6 Hz to 10.6 Hz.

Table 1. The nonlinear and underlying linear parameters

Mass $m = 1.5\ kg$, Damping coefficient $c = 0.8\ Ns/m$, $k = 6000\ N/m$			
Nonlinearity	Damping f_c	Stiffness f_k	*Values*
Duffing Oscillator	0	$f_k = k_{nl}\ x^3$	$k_{nl} = 7\ 10^6\ N/m^3$
Quadratic damping	$f_c = c_{nl}\dot{x}\lvert\dot{x}\rvert$	0	$c_{nl} = 8\ Ns^2m^{-2}$
Coulomb damping	$f_c = F_f sgn(\dot{x})$	0	$F_f = 0.85$
cubic stiffness +	$f_c = c_{nl}\dot{x}\lvert\dot{x}\rvert$	$f_k = k_{nl}\ x^3$	$k_{nl} = 7\ 10^6\ N/m^3$
Quadratic damping			$c_{nl} = 8\ Ns^2/m^2$

Figure 2 depicts the response of the system excited for several levels from 1.10^{-2} to 4.10^{-2} mm with a step of 1.10^{-2} mm. It is notable that the resonance frequency shifts up to higher frequencies with the increase of the level of excitation. It is clearly observed that the system has a hardening behavior and this is consistent with the sign of the cubic coefficient ($k_{nl} > 0$). At higher excitations, the jump phenomenon will be clearly visible and hence the nonlinearity will be stronger.

2.2.2. Coulomb damping

Let's consider the nonlinear system with coulomb damping specified by the equation of motion:

$$m\ddot{z} + c\dot{z} + F_f sgn(\dot{z}) + kz = \omega^2 mY \sin(\omega t) \tag{15}$$

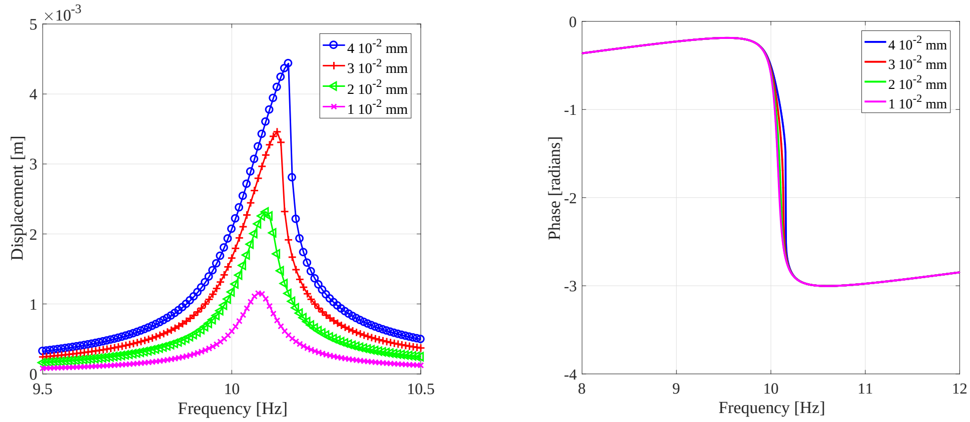

(a) Amplitude (b) Phase

Figure 2. The response of the Duffing Oscillator system for different levels of excitation

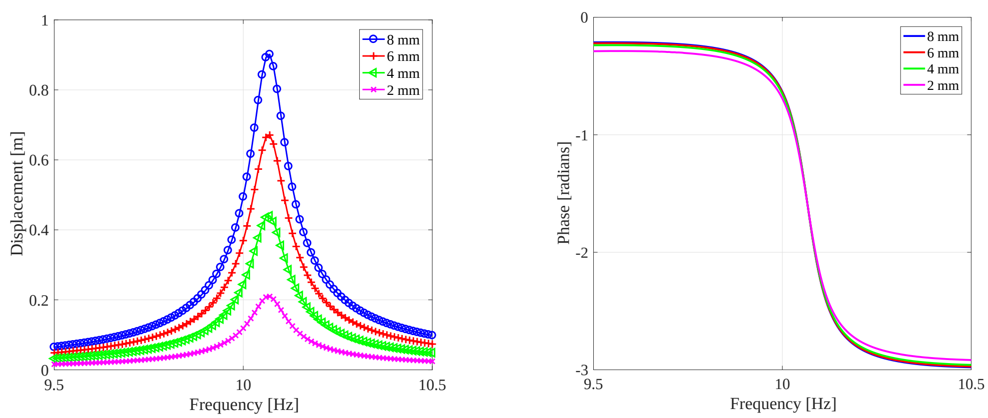

(a) Amplitude (b) Phase

Figure 3. The response of the coulomb damping system for different levels of excitation

where sgn represents the sign function which is defined as follows:

$$sgn\,(x) = \begin{cases} -1 & if \quad x < 0 \\ 0 & if \quad x = 0 \\ 1 & if \quad x > 0 \end{cases} \tag{16}$$

The displacement response was obtained by setting the excitation frequency from 9.6 Hz to 10.6 Hz and increasing the level of excitation from 2 mm to 8 mm. This increase induces the increase of the resonance amplitude from 0.2 m up to 0.85 m. Contrary to the previous type of nonlinearity, the system behaves nominally linearly at high excitation. In the case of Coulomb damping system, the nonlinearity is only visible if the level of excitation is low.

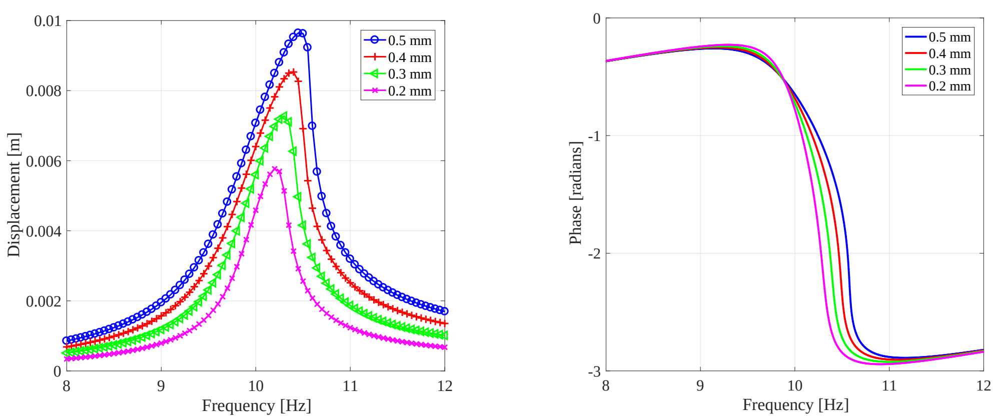

(a) Amplitude (b) Phase

Figure 4. The response of the combined cubic stiffness and quadratic damping system for different levels of excitation

2.2.3. *Combined nonlinearities: Cubic stiffness and quadratic damping*

Another system, which is an interesting physical system and most studied in the nonlinear engineering, combined cubic stiffness and quadratic damping will be studied. In this case, the equation of motion is given by:

$$m\ddot{z} + c\ \dot{z} + c_{nl}\dot{z}|\dot{z}| + k\ z + k_{nl}z^3 = \omega^2 mY \sin(\omega t) \tag{17}$$

The presented systems response, under harmonic excitation of the base, for different amplitudes are presented in Figure 4. From the figure, it is interesting to note that the raised excitation level obviously causes the increase of the resonance frequency. Meanwhile, the jump phenomenon observed at higher level of excitation while no obvious jump phenomenon occurs at lower excitation. This means that the system performs as hardening stiffness under large deformation and nearly unchanged under small deformation.

3. Numerical validations

The third section aims to evaluate the efficiency of the proposed method by comparing the identified results with analytical expressions for stiffness and damping functions.

3.1. Analytical stiffness and damping functions

The analytical stiffness and damping functions have been derived using the Harmonic Balance Method to solve the nonlinear equation of motion (Worden and Tomlinson, 2000).

In fact, the analytical expressions correspond to the stiffness and damping of a linearized system under the assumption that the system responds at the same frequency as the harmonic excitation. This is equivalent to expressions determined by applying the first-order expansion using Harmonic Balance approximation in the steady state.

3.1.1. Nonlinear Stiffness

The analysis will be simplified by considering the motion equation of a simple oscillator subjected to a harmonic excitation as:

$$m\ddot{y} + c\dot{y} + f_s(y) = x(t) \tag{18}$$

where f_s represents nonlinear stiffness function.

Assuming that the nonlinear stiffness is equal to the equivalent stiffness:

$$f_s(y) \approx K_{eq} y \tag{19}$$

The harmonic balance trial solution $Y \sin(\omega t)$ yields the nonlinear form $f_s(Y \sin(\omega t))$. This function can be expanded using the Fourier series and only the fundamental term (first harmonic) is considered. So,

$$f_s(Y \sin(\omega t)) \approx b_1 \sin(\omega t) = K_{eq} Y \sin(\omega t) \tag{20}$$

where b_1 represents the Fourier coefficient of the fundamental term. The mathematical model of a cubic stiffness element can be expressed as

$$f_s(y) = ky + k_{nl}y^3 \tag{21}$$

The first integration gives the linear part and the contribution from the nonlinear stiffness is $\frac{3}{4}\ k_{nl}\ Y^2$, so:

$$K_{eq} = k + \frac{3}{4}k_{nl}Y^2 \tag{22}$$

where k and k_{nl} represent the linear parameter and the nonlinear parameter, respectively.

3.1.2. Nonlinear Damping

The formulas presented above are limited to the case of nonlinear stiffness. It is possible to extend its application to nonlinear damping. Let's consider the following system.

$$m\ddot{y} + f_d(\dot{y}) + ky = x(t) \tag{23}$$

where f_d denotes the nonlinear damping function. Choosing a trial output solution $Y\sin(\omega t)$ yields a nonlinear function $f_d(\omega Y\cos(\omega t))$. This function can be rewritten as follow:

$$f_d(\omega Y\cos(\omega t)) = a_1\cos(\omega t) = C_{eq}\omega Y\cos(\omega t) \tag{24}$$

where a_1 is the Fourier coefficient of the fundamental term. The mathematical model of a quadratic damping element can be expressed as:

$$f_d(\dot{y}) = c\dot{y} + c_{nl}\dot{y}|\dot{y}| \tag{25}$$

Then, the equivalent damping is given by:

$$C_{eq} = \frac{c}{\omega Y\pi}\int_0^{2\pi}\omega Y\cos\theta\cos\theta d\theta + \frac{c_{nl}}{\omega Y\pi}\int_0^{2\pi}\omega Y\cos\theta|\omega Y\cos\theta|\cos\theta d\theta \tag{26}$$

After integration, this becomes:

$$C_{eq} = c + \frac{8}{3\pi}c_{nl}\omega Y \tag{27}$$

where ω is the natural frequency of the linear system and Y is the amplitude of the response at steady state. c and c_{nl} represent the linear and the non-linear damping parameters, respectively.
Similarly, for the case of coulomb damping:

$$f_d(\dot{y}) = c \quad \dot{y} + c_F \quad \frac{\dot{y}}{|\dot{y}|} = c\dot{y} + c_F \quad sign(\dot{y}) \tag{28}$$

The equivalent damping is defined as:

$$C_{eq} = c + \frac{4}{\pi}\frac{F_f}{\omega Y} \tag{29}$$

where F_f is the coulomb force.

3.2. Comparison with analytical equivalent expressions

In order to validate the proposed method, three classical types of nonlinear systems, presented above, are used in this section as examples for the numerical validation study. The nonlinear stiffness and damping are calculated using Eq. (10) and will be identified with special functions by means of the curve fitting technique. Tables 2-4 present these polynomial fit functions compared to their analytic expressions. The analytical stiffness and damping expressions are demonstrated for each case in the previous section.

3.2.1. Combination of quadratic damping and cubic stiffness

The first case corresponds to a SDOF system with a combination of cubic stiffness and quadratic damping. Results are calculated using the fourth order Runge-Kutta method for frequency range between 8 Hz and 12 Hz with frequency increments of 0.05 Hz. The stepped-sine base excitations are allowed to vary from 2 mm to 5 mm with a step of 1 mm for each frequency. From results shown in the Figures (5(a) and 5(b)), a systematic increase in the natural frequency clearly depicts a hardening behavior of the nonlinearity and therefore the terms of mathematical functions can be identified by mean of fitting the corresponding data.

Table 2. Identified parameters for a system with combined nonlinearities

	Ideal expressions	Identified results	Goodness of fit
Stiffness	$K_{eq} = 6 \quad 10^3 + \frac{3}{4} \; 710^6 \;\; X^2$	$K_{fit} = 6001.6 + \frac{3}{4} \; 7.0397 \;\; 10^6 \;\; X^2$	0.9999
Damping	$C_{eq} = 0.8 + \frac{8}{3\pi} \;\; 8 \;\; \omega X$	$C_{fit} = 0.82884 + \frac{8}{3\pi} \;\; 7.9388 \;\; \omega X$	0.9997

As it can be seen from Table 2, the least-squares fitting of the identified nonlinear results characteristics to a mathematical model returns the nonlinear stiffness coefficient that is equal to $\frac{3}{4} \;\; 7.0631 \;\; 10^6$ when the equivalent stiffness coefficient is equal to $\frac{3}{4} \;\; 7 \;\; 10^6$. The estimated nonlinear damping coefficient is equal to $\frac{8}{3\pi} \;\; 8.0805$ when the equivalent damping coefficient is equal to $\frac{8}{3\pi} \;\; 8$. The comparison between the identified and the analytical expression clearly shows that the proposed approach reaches a precise estimation as indicated by the goodness of fit with values of 0.9999 and 0.9997.

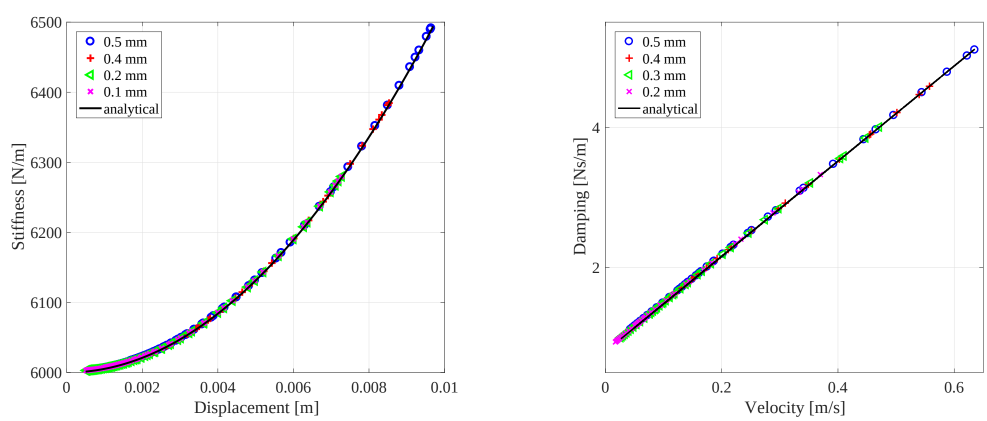

(a) Stiffness (b) Damping

Figure 5. Comparison between the estimated stiffness and damping functions and the analytical equivalent functions: System with combined cubic stiffness and quadratic damping

3.2.2. *Dry friction: Coulomb damping*

Using the transmissibility curves obtained for the frequency range of 8 to 12 Hz with a step of 0.005 Hz and for several amplitudes of excitation ranging between 8 mm and 2 mm with step of 2 mm, the information on the nonlinearities are given in Figures (6(a) and 6(b)). It can be seen that by increasing the amplitude, the stiffness remains constant, while the damping decreases with hyperbolic trend (due to the Coulomb damping). From results in Table 3, a good agreement is reached between the identified function and the appropriated analytical expression. The error is less than 0.4 % between the identified coulomb damping and the equivalent coefficients.

Table 3. Identified parameters for the system with Coulomb friction

	Ideal expressions	Identified results	Goodness of fit
Stiffness	$K_{eq} = 6 \ \ 10^3$	$K_{fit} = 6.001 \ \ 10^3$	0.9998
Damping	$C_{eq} = 0.8 + \frac{8}{3\pi} \ 0.85 \ (\omega X)^{-1}$	$C_{fit} = 0.8208 + \frac{8}{3\pi} \ 0.8498 \ (\omega X)^{-0.9991}$	0.9970

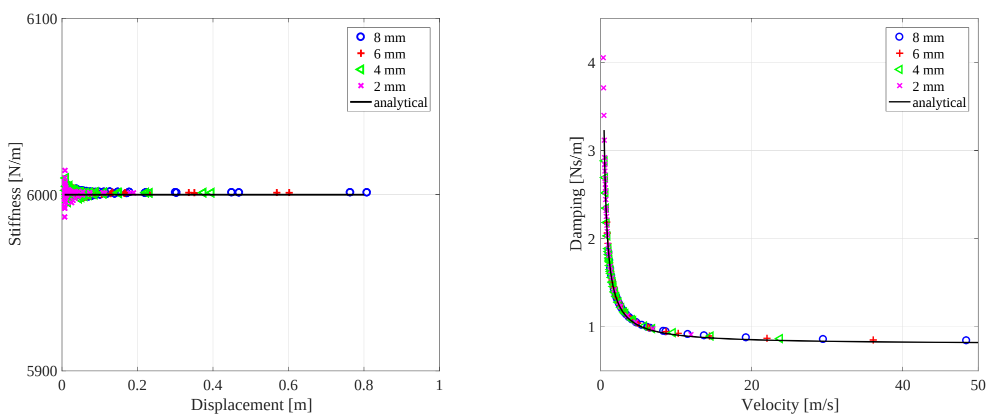

(a) Stiffness

(b) Damping

Figure 6. Comparison between the estimated stiffness and damping functions and the analytical equivalent functions: System with Coulomb damping

3.2.3. Duffing oscillator: Cubic stiffness

A SDOF system with Duffing oscillator is now investigated. To estimate the stiffness and damping curves, the required response record is generated within the frequency excitation range from 8 Hz to 12 Hz. Figure 7 shows the results of the analysis of the transmissibility of a system with coulomb damping under harmonic base excitations. The amplitude of the base excitation are ranging between 1 $10^{-}2$ mm and 4 $10^{-}2$ mm with an increment of 1 $10^{-}2$ mm. The left hand panel shows that by increasing the amplitude of response, there is a consistent increase in natural frequency, due to the hardening behavior.

Table 4. Identified parameters for the Duffing oscillator

	Ideal expressions	Identified results	Goodness of fit
Stiffness	$K_{eq} = 6 \quad 10^3 + \frac{3}{4} \; 710^6 \; X^2$	$K_{fit} = 6002.5 + \frac{3}{4} \; 7.7072 \; 10^6 \; X^2$	0.9988
Damping	$C_{eq} = 0.8$	$C_{fit} = 0.8206$	0.9998

Meanwhile, an accurate prediction of the stiffness is achieved by implementing a successful estimation using the proposed method. The identified stiffness do not deviate more than 4.7 % from the ideal function, as presented in Table 4. It is interesting to note that the right panel of Figure 7 shows slight differences when the identified damping is compared to the analytic expression.

Results show a good match between both approaches when estimating the stiffness and damping in the case of strong nonlinearities. This reveals the effectiveness of the method presented in this paper and offers the possibility to implement the approach for real experimental measurements.

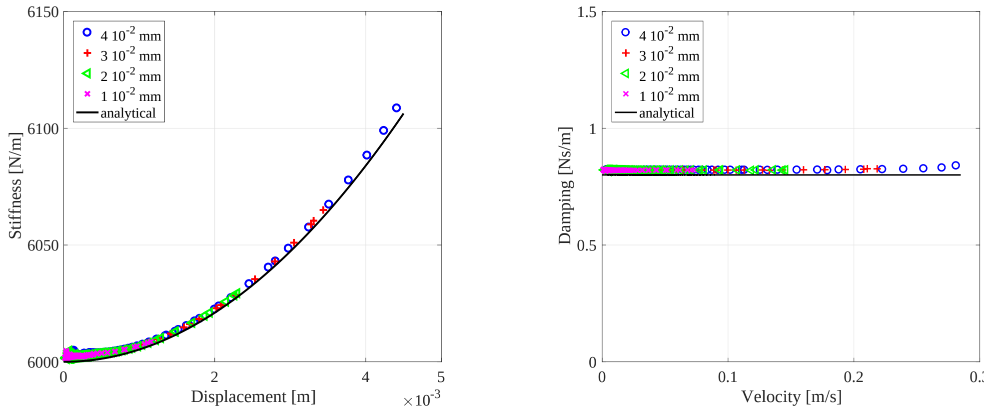

(a) Stiffness (b) Damping

Figure 7. Comparison between the estimated stiffness and damping functions and the analytical equivalent functions: System with Duffing oscillator

4. Application of the proposed approach on the metal mesh isolator and comparison of the measurements with predictions

To validate and demonstrate the applicability of the identification procedure given above, experimental tests were performed on commercial metal mesh isolator. The experimental set up is displayed in Figure 8.

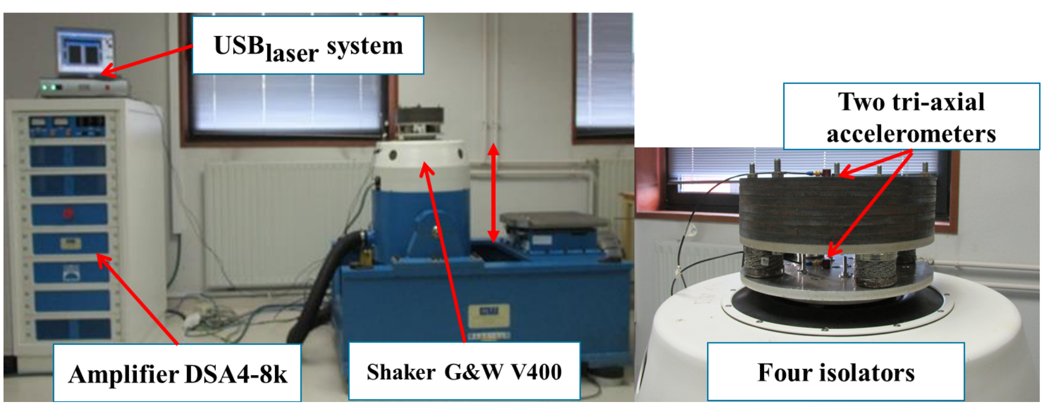

Figure 8. Experimental set-up

The electro-dynamic shaker, Gearing and Watson V400, was driven by a signal generator producing a stepped-sine signal. The accelerometers (ENDEVCO, model 65M100) were rigidly attached to the shaker-table and to the mass plate to measure the input-output data, while the Dactron associated software was used to observe the system response. The data were recorded using a $LASER_{USB}$ shaker control system connected to a computer. The bottom of the damper is connected to the base whereas the top is connected to the rigid mass weighed about 30 kg. The test rig is designed to measure the transmissibility using four vibration isolators of the same model. The tests were repeated three times to ascertain variability of the experimental data and only the average curves are considered during the investigation. The magnitude and phase of the transmissibility for excitation levels of 2 m/s^2 and 3 m/s^2, are depicted in Figures (9(a) and 9(b)). The metal mesh isolator essentially consists of a cushion of stainless steel, woven using a knitting machine, rolled and/or pressed into the required geometric shape via a press mold in order to achieve the desired geometric shape, so that different geometries can be manufactured depending on the application by changing the mold process. It was produced with an relative density of 24.93 %.

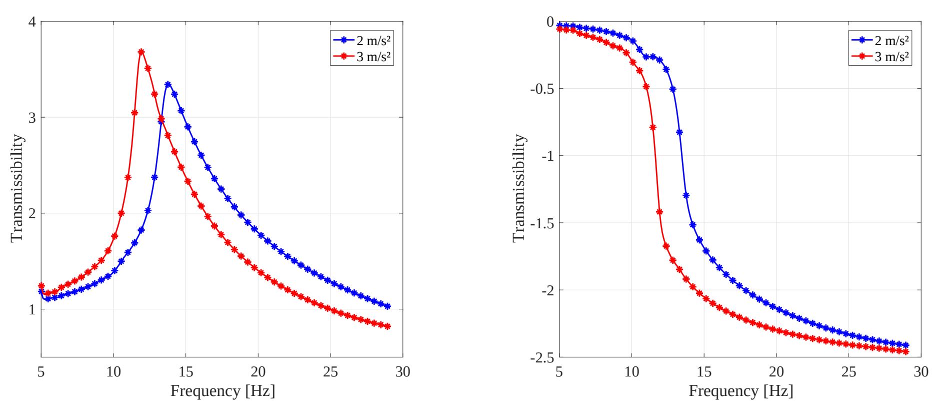

(a) Amplitude (b) Phase

Figure 9. Acceleration responses to stepped-sine excitation of different amplitudes (a) amplitude responses and (b) phase responses

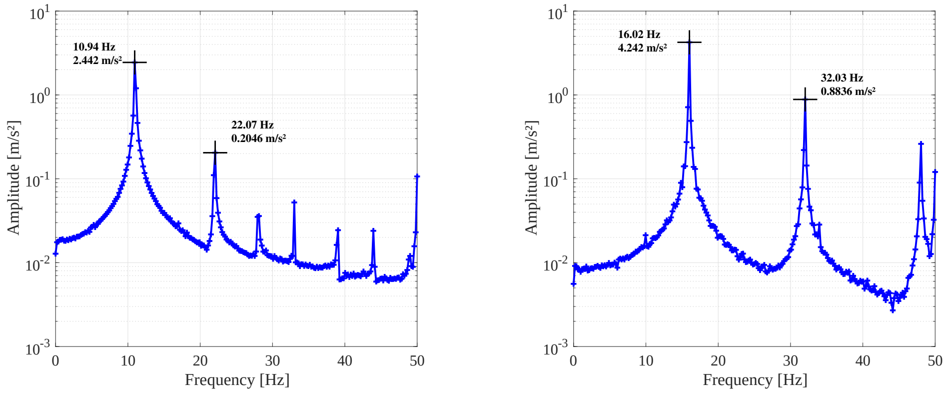

(a) 11 Hz (b) 16 Hz

Figure 10. The spectrum of the response

The spectrum of the response of the isolator at 11 Hz and 16 Hz are shown in Figure 10. It is worth noticing that the sub- and super-harmonics of the response in each stepped-sine are much less than 5% of the primary harmonic component (Figure 10(b)). Thus, the response of the system is dominated by the fundamental harmonic component and higher harmonic components can be ignored. Therefore, the assumption of the primary harmonic component on the solution in Eq.(4) is reasonable and accurate.

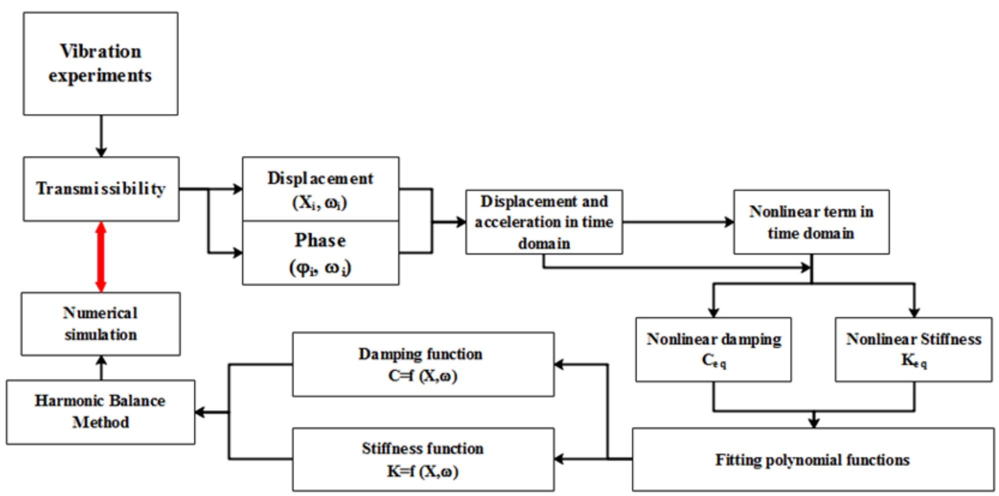

Figure 11. Flowchart of the proposed method

A flowchart of the proposed method is shown in Figure 11, where the thick line denote the comparison between the numerical simulations and experimental data. Figure 12 presents the stiffness and damping maps of damper-model including the calculated points using the proposed identification method and the identified surfaces. The least squares polynomial approximation, via surface fitting MATLAB toolbox, were used during the identification. In order to reach a good fit for stiffness and damping, the order and type of the basic functions will be chosen by comparing the fitting results of different ordinary polynomials. Increasing the polynomial terms order increases the complexity of the mathematical model; however, the fit quality is slightly improved.

The basic function of the stiffness is obtained by substituting $N_1 = 3$, $N_2 = 0$ and $i + j < 3$ in Eq. (11), however, the damping basic function is obtained by choosing $N_1 = 4$, $N_2 = 2$ and $i + j < 4$ in Eq. (12):

$$B_{ij}^{Stiff}(X, \omega) = 1, X, X^2, X^3 \tag{30}$$

$$B_{ij}^{Damp}(X, \omega) = 1, X, \omega, X\omega, X^3, X^2\omega, X\omega^2, X^4, X^3\omega, X^2\omega^2 \tag{31}$$

Therefore, the nonlinear stiffness mathematical model could be written as:

$$K(X, \omega) = 1.60710^5 - 2.77710^8 X + 2.52510^1 1X^2 - 7.97510^1 3X^3 \tag{32}$$

where the goodness of fit is 0.9661.

Also, the damping model expressed as:

$$\begin{gathered} C(X, \omega) = 1090 - 1.19110^7 X + 3.14810^2 \omega + 3.09510^5 X\omega \\ -5.04210^1 1X^3 - 8.23410^8 X^2\omega - 2073X\omega^2 - 1.311610^1 4X^4 \\ +1.08610^1 0X^3\omega + 5.39710^6 X^2\omega^2 \end{gathered} \tag{33}$$

where the goodness of fit is 0.9585.

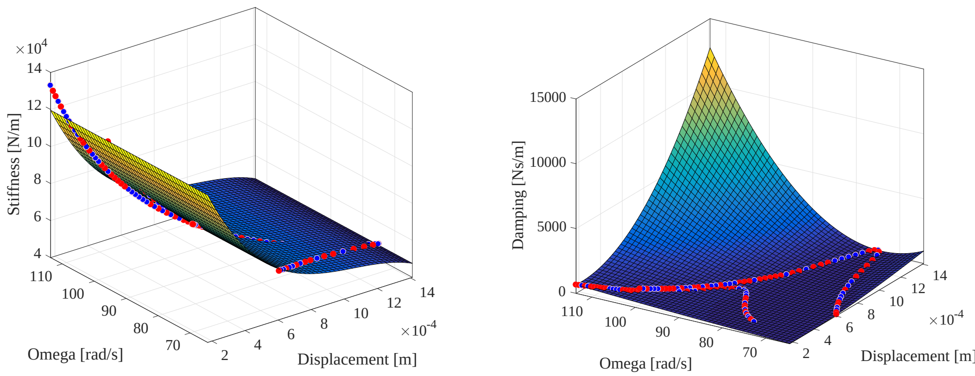

(a) Stiffness

(b) Damping

Figure 12. a) Stiffness and b) damping map of metal mesh damper including calculated points from measured data

With identified coefficients of the stiffness and damping models, the relative transmissibility at these two excitation amplitudes (2 m/s^2 and 3 m/s^2) can be predicted by solving iteratively:

$$T_r(X,\omega) = |\frac{\omega^2}{\omega_0^2(X,\omega) - \omega^2 + j\eta(X,\omega)\omega_0^2(X,\omega)|} \tag{34}$$

where $\omega_0(X,\omega)$ and $\eta(X,\omega)$ are the nature frequency and loss factor, respectively and can be calculated from:

$$\begin{aligned} K(X,\omega) &= \omega_0^2(X,\omega)m \\ C(X,\omega) &= \eta(X,\omega)\omega_0^2(X,\omega)m \end{aligned} \tag{35}$$

Figures (13(a) and 13(b)) show the comparison between the predicted and measured transmissibility. Good match of correlation between the predicted and measured data is reached. However, the predicted resonant frequency and peak marked in Figure 13(a) are a little lower than the measured ones. This slight error can be explained by the limitation in the surface fitting tools of MATLAB and some other more complicated damping that may appear.

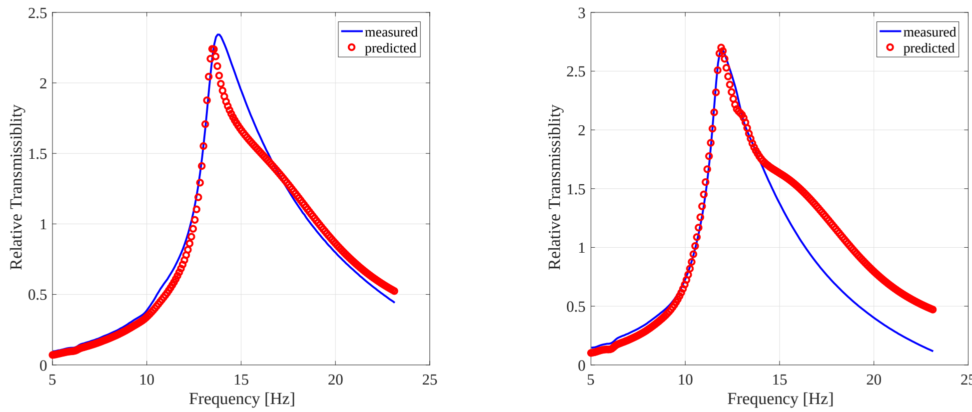

(a) 2 m/s^2 (b) 3 m/s^2

Figure 13. Comparison between measured and identified responses

5. Application using multi-harmonic excitation

The identification of SDOF systems parameters, using mono-harmonic excitation, is demonstrated by both numerical and experimental examples in previous sections. In this part, the proposed identification technique will be extended to identify nonlinearity from SDOF systems subjected to multi-harmonic excitations. This example is used to demonstrate the efficiency of the identification method while employing multi-harmonic excitation in place of one-harmonic.
The equation of motion can be rewritten in the matrix form:

$$m\ddot{X} + F_{nl}(X, \dot{X}) = F_e \tag{36}$$

where

$$F_{nl}(X, \dot{X}) = C_{eq}\dot{X} + K_{eq}X \tag{37}$$

As the excitation terms is periodic, it is assumed that the nonlinear dynamical response and the force vector may be approximated by finite Fourier series with ω as fundamental frequency.

$$X(t) = \sum_{n=1}^{N} X_{\cos}^{(n)} \cos(n\omega t) + X_{\sin}^{(n)} \sin(n\omega t)$$
$$F_{nl}(t) = \sum_{n=1}^{N} F_{\cos}^{(n)} \cos(n\omega t) + F_{\sin}^{(n)} \sin(n\omega t)$$
$$F_{e}(t) = \sum_{n=1}^{N} F_{e_{\cos}}^{(n)} \cos(n\omega t) + F_{e_{\sin}}^{(n)} \sin(n\omega t)$$

where $(X_{\cos}^{(n)}, X_{\sin}^{(n)})$, $(F_{\cos}^{(n)}, F_{\sin}^{(n)})$ and $(F_{\cos}^{(n)}, F_{\sin}^{(n)})$ are Fourier coefficients of the displacement, restoring force and excitation force, respectively.

In this work, a two-harmonic input (N=2) is considered for the identification (Figure 14) and a comparative study on the success of identication is carried out. Let's consider the system subjected to two harmonic excitations.

$$-m\omega^2 \begin{Bmatrix} X_{\cos}^{(1)} \\ X_{\sin}^{(1)} \\ 4X_{\cos}^{(2)} \\ 4X_{\sin}^{(2)} \end{Bmatrix} + C_{eq}\omega \begin{Bmatrix} X_{\sin}^{(1)} \\ -X_{\cos}^{(1)} \\ 2X_{\sin}^{(2)} \\ 2X_{\cos}^{(2)} \end{Bmatrix} + K_{eq} \begin{Bmatrix} X_{\cos}^{(1)} \\ X_{\sin}^{(1)} \\ X_{\cos}^{(2)} \\ X_{\sin}^{(2)} \end{Bmatrix} = \begin{Bmatrix} F_{e_{\cos}}^{(1)} \\ F_{e_{\sin}}^{(1)} \\ F_{e_{\cos}}^{(2)} \\ F_{e_{\sin}}^{(2)} \end{Bmatrix} \tag{38}$$

From Eq. (36), the restoring force can be written as:

$$\begin{Bmatrix} F_{\cos}^{(1)} \\ F_{\sin}^{(1)} \\ F_{\cos}^{(2)} \\ F_{\sin}^{(2)} \end{Bmatrix} = \begin{Bmatrix} F_{e_{\cos}}^{(1)} \\ F_{e_{\sin}}^{(1)} \\ F_{e_{\cos}}^{(2)} \\ F_{e_{\sin}}^{(2)} \end{Bmatrix} + m\omega^2 \begin{Bmatrix} X_{\cos}^{(1)} \\ X_{\sin}^{(1)} \\ 4X_{\cos}^{(2)} \\ 4X_{\sin}^{(2)} \end{Bmatrix} \tag{39}$$

Thus, the equivalent stiffness and damping could be obtained by measurement of the restoring force and displacement responses.

$$\begin{Bmatrix} F_{\cos}^{(1)} \\ F_{\sin}^{(1)} \\ F_{\cos}^{(2)} \\ F_{\sin}^{(2)} \end{Bmatrix} = \begin{bmatrix} X_{\cos}^{(1)} & \omega X_{\sin}^{(1)} \\ X_{\sin}^{(1)} & -\omega X_{\cos}^{(1)} \\ X_{\cos}^{(2)} & 2\omega X_{\sin}^{(2)} \\ X_{\sin}^{(2)} & -2\omega X_{\cos}^{(2)} \end{bmatrix} \begin{Bmatrix} K_{eq} \\ C_{eq} \end{Bmatrix} \tag{40}$$

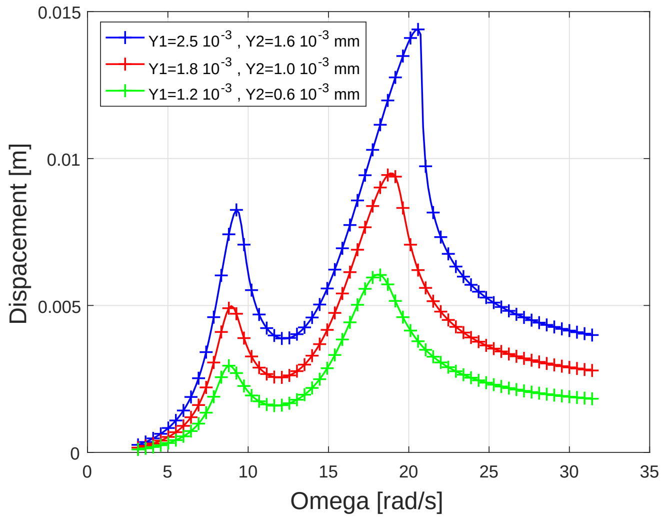

Figure 14. Response of SDOF excited by two harmonic excitations

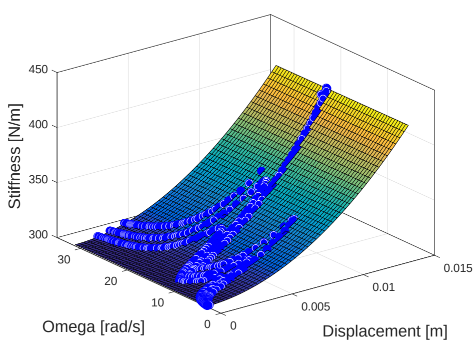

(a) Three dimensional view

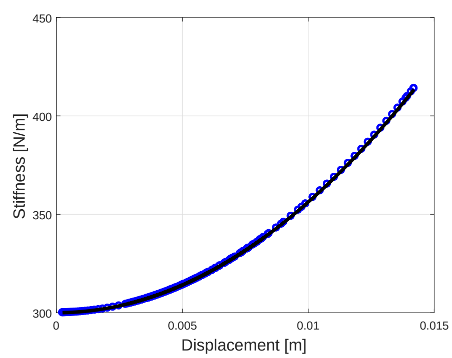

(b) Projection of the map

Figure 15. Stiffness of the two-harmonic excited system with Duffing oscillator

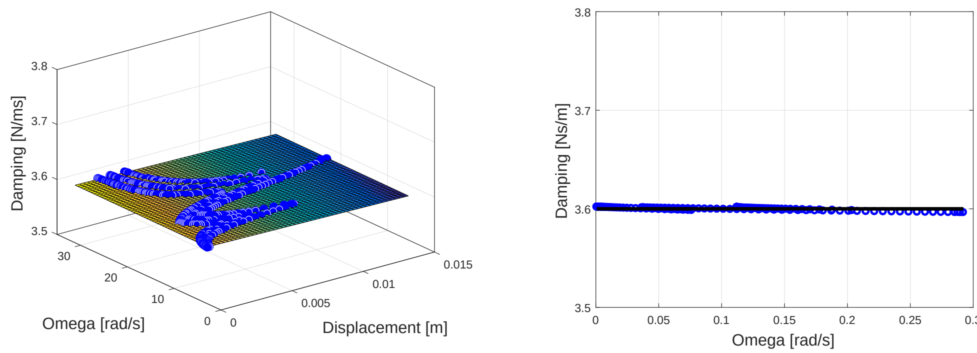

(a) Three dimensional view (b) Projection of the map

Figure 16. Damping of the two-harmonic excited system with Duffing oscillator

The proposed identification technique is used to identify the unknown parameters of the SDOF system with Duffing oscillator where the equation of motion is given by:

$$m\ddot{x} + c\dot{x} + kx + f_c(\dot{x}) + f_k(x) = m\ \omega^2\ Y_1\ sin(\omega t) + m\ (2\omega)^2\ Y_2\ sin(2\omega t) \quad (41)$$

Table 5. Two-harmonic excitation: parameter setting for simulation

Mass $m = 1\ kg$, Damping coefficient $c = 3.6\ Ns/m$, $k = 300\ N/m$			
Nonlinearity	Damping f_c	Stiffness f_k	*Values*
Duffing Oscillator	0	$f_k = \alpha\ x^3$	$\alpha = 7.5\ 10^5\ N/m^3$

The parameters used in the simulation are given in Table 5. The results, shown in Figures 15 and 16, give a much correlation in the term of predicted results; it could be seen that the estimation of linear stiffness coefficient (less than 0.46 % error), cubic stiffness coefficient (less than 1.31 % error) and linear damping coefficient (less than 0.44 % error) of the unknown elements are accurate compared to the exact values (Table 6). Thus, the Alternating Frequency Time Domains identification technique is still efficient for systems subjected to multi-harmonic excitations.

Table 6. Identified parameters for a system with combined nonlinearities

	Ideal expressions	Identified results	Goodness of fit
Stiffness	$K_{eq} = 300 + \frac{3}{4}\ 7.5\ 10^5\ X^2$	$K_{fit} = 298.6 + \frac{3}{4}\ 7.5987\ 10^5\ X^2$	0.9988
Damping	$C_{eq} = 3.6\ \omega$	$C_{fit} = 3.616\ \omega$	0.9956

Conclusion

A nonparametric technique for the identification of nonlinear systems has been proposed by alternating between the frequency and time domains. This procedure is developed to extract the stiffness and damping that depend on the response amplitude and frequency, and thus these points will be plotted as discrete points. The mathematical model of the system is obtained and unknowns parameters are identified by surface fitting these points. Numerical examples and then real experimental example demonstrate the effectiveness and accuracy of the identified results with this technique. Good agreements are reached between the predicted and measured results. Finally, an application of the method to SDOF system subjected to multi-harmonic excitations is also illustrated.
The contribution of this paper is the development of a new methodology for the characterization of the nonlinear behavior and the identification of unknown parameters of a commercial vibration isolator. The objective of this method is to define a mathematical model to provide a better understanding of the real system characterization. The developed model consists on predicting the response of the isolator under different excitation amplitudes. In addition, the assumption considering only the primary harmonic can be extended to include the super- and sub-harmonics. Besides, this technique is applied to identify the linear and nonlinear parts using ordinary polynomials and no prior information about the nonlinearity is required. Thus, the method can provide reliable model of the complex nonlinear system. However, this technique has also some limitations. The estimated damping-model, expressed in polynomial form, has no physical meaning. So, the physical constrictive model must be taken into consideration. That is to say, the combination of

different types of nonlinearities, such as viscous damping, coulomb damping and quadratic damping, should be reflected in the identification of damping.

References

Al-Hadid, M.A., Wright, J., 1989. Developments in the force-state mapping technique for non-linear systems and the extension to the location of non-linear elements in a lumped-parameter system. Mechanical Systems and Signal Processing3, 269–90.

Aykan, M., Özgüven, H.N., 2012. Parametric identification of nonlinearity from incomplete frf data using describing function inversion, in: Topics in Nonlinear Dynamics, Volume 3. Springer, pp. 311–22.

Aykan, M., Özgüven, H.N., 2013. Parametric identification of nonlinearity in structural systems using describing function inversion. Mechanical Systems and Signal Processing40, 356–76.

Carrella, A., 2012. Nonlinear identifications using transmissibility: Dynamic characterisation of anti vibration mounts (avms) with standard approach and nonlinear analysis. International Journal of Mechanical Sciences63, 74–85.

Carrella, A., Ewins, D., 2011. Identifying and quantifying structural nonlinearities in engineering applications from measured frequency response functions. Mechanical Systems and Signal Processing25, 1011–27.

Dittman, E.R., 2013. Identification and quantification of nonlinear behavior in a disbonded aluminum honeycomb panel using single degree-of-freedom models. Ph.D. thesis. Purdue University.

Feldman, M., 1994a. Non-linear system vibration analysis using hilbert transform–i. free vibration analysis method'freevib'. Mechanical systems and signal processing8, 119–27.

Feldman, M., 1994b. Non-linear system vibration analysis using hilbert transform–ii. forced vibration analysis method'forcevib'. Mechanical Systems and Signal Processing8, 309–18.

Guo, P., 2012. Damping system designs using nonlinear frequency analysis approach.

Kerschen, G., Worden, K., Vakakis, A.F., Golinval, J.C., 2006. Past, present and future of nonlinear system identification in structural dynamics. Mechanical systems and signal processing20, 505–92.

Lin, R., 1990. Identification of the dynamic characteristics of nonlinear structures. Diss. University of London.

Masri, S., Caughey, T., 1979. A nonparametric identification technique for nonlinear dynamic problems. Journal of Applied Mechanics46, 433–47.

Mezghani, F., Del Rincón, A.F., Souf, M.A.B., Fernandez, P.G., Chaari, F., Rueda, F.V., Haddar, M., 2017. Identification of nonlinear anti-vibration isolator properties. Comptes Rendus Mécanique345, 386–98.

Özer, M.B., Özgüven, H.N., 2002. A new method for localization and identification of non-linearities in structures, in: Proceedings of ESDA 2002: 6th Biennial Conference on Engineering Systems Design and Analysis, pp. 8–11.

Özer, M.B., Özgüven, H.N., Royston, T.J., 2009. Identification of structural non-linearities using describing functions and the sherman–morrison method. Mechanical Systems and Signal Processing23, 30–44.

Schetzen, M., 1980. The volterra and wiener theories of nonlinear systems.

Volterra, V., 2005. Theory of functionals and of integral and integro-differential equations. Courier Corporation.

Wang, X., Zheng, G., 2016. Equivalent dynamic stiffness mapping technique for identifying nonlinear structural elements from frequency response functions. Mechanical Systems and Signal Processing68, 394–415.

Wiener, N., 1942. Response of a non-linear device to noise. Technical Report. Massachusetts Inst Of Tech Cambridge Radiation Lab.

Worden, K., Tomlinson, G.R., 2000. Nonlinearity in structural dynamics: detection, identification and modelling. CRC Press.